Ultrasound-guided, open-source microneurography: Approaches to improve recordings from peripheral nerves in man.

James P. Dunham a,b*, Anna C. Sales a and Anthony E. Pickering a,b.

a - School of Physiology, Pharmacology & Neuroscience, University of Bristol, Bristol, United Kingdom.

b - Anaesthesia, Pain & Critical Care Sciences, Translational Health Sciences, Bristol Medical School, University of Bristol, BS2 8HW.

Corresponding author (*) James.P.Dunham@Bristol.ac.uk

Funding: This work was supported by the National Institute for Health Research and Wellcome Trust [gr088373]. JPD is an NIHR Academic Clinical Fellow.

Structured abstract
Objective
Microneurography is the only method for recording from single neurons in intact human nerves. It is challenging - requiring technical expertise, investment in specialised equipment and has sparse data yields.

Methods
We assessed whether ultrasound guidance in combination with an 'open access' amplifier and data capture system (Open-Ephys) would simplify and expand the scope of microneurographic recordings in humans.

Results
In 32 healthy consenting volunteers, ultrasound-guidance improved success rates for obtaining cutaneous C-fibres and reduced "Skin to Nerve" times from 28.5 minutes to 4.5 minutes for recordings of the peroneal nerve ($P<0.0001$).

We illustrate the potential utility of ultrasound-guided microneurography for difficult to access nerves with phrenic nerve recording during a Valsalva manoeuvre.

We show that Open Ephys is a viable alternative to commercially available recording systems and offers advantages in terms of cost and software customisability.

Conclusions
Ultrasound guidance for microneurography with Open Ephys facilitates cutaneous C nociceptor recordings and allows recordings to be made from nerves previously considered inaccessible.

Significance
We anticipate that the adoption of these techniques will improve microneurography experimental efficiency, adds an important visual learning aid and increases the generalisability of the approach.

Keywords: Microneurography, Pain, C-fibre, Nociceptor, Open-source, Ultrasound.

Highlights
Ultrasound-guided microneurography improves data yields and reduces experimental duration.
Open Ephys, an open source data acquisition system, offers advantages for human microneurography.
Ultrasound with OpenEphys will facilitate targeted microneurography based upon clinical presentation.

1. Introduction

Microneurography is an established technique that allows recordings to be made from peripheral nerves in humans (Vallbo and Hagbarth, 1968, Vallbo et al. , 2004). This includes the ability to record from afferent neurones conducting in the C-fibre range (Torebjork and Hallin, 1974), which are predominantly nociceptors. In the pain field, the normal response characteristics of several classes of nociceptors have been defined

and a growing body of work is now identifying pathophysiological changes in human disease (Donadio and Liguori, 2015).

Despite these advances and many decades of use, microneurography remains challenging. In the words of the developers of the technique, ".. experiments are time consuming and demanding for both the experimenter and the subject, particularly when the aim is to study single-unit activity. Short recording sessions may be preceded by long search periods requiring maximal attention to delicate visual and auditory cues while the experimenter has to make minute manual adjustments of the electrode position." (Vallbo et al. , 2004). An additional difficulty is the expense and relative paucity of choice of available hardware and software which is either custom built/written or available from only a handful of suppliers commercially.

The use of ultrasound to aid the placement of microneurography electrodes has been reported (Curry and Charkoudian, 2011, Granata et al. , 2016). Curry and Charkoudian targeted the common peroneal, ulnar, median and radial nerves (large nerves commonly targeted by microneurographers) in order to make recordings of muscle sympathetic nerve activity (MSNA). Promisingly, they reported that "time to placing the microelectrode into the nerve can be reduced to just a few minutes" however, no quantitative data were presented and it is unclear how many participants were involved in their study. A letter subsequently suggested that higher frequency ultrasound scan rates can improve electrode visualisation during microneurography based on a single case at the median nerve (Granata et al. , 2016).

We wished to use microneurography to record from cutaneous C fibre nociceptors innervating the skin of the lower limb. In seeking to optimise our technique we compared the traditional technique of recording from the common peroneal nerve (CPN-a mixed nerve) at the fibular head, with ultrasound guided electrode placement in the superficial peroneal nerve (SPN-a small, cutaneous nerve) targeted in the lower leg. In principle, the SPN in the lower leg should yield a higher proportion of cutaneous C fibre recordings as it lacks the motor fascicles or sensory innervation of deeper structures. These principles have been borne out previously with targeting of the SPN at the ankle, see (Serra et al. , 2004) for example.

Furthermore, it has been suggested that researchers may sub optimally place their electrodes in order to facilitate visualisation of the electrode when using ultrasound. This could then lead to unstable recordings (McNulty and Hodson-Tole, 2016). To address this possibility, we also compared ultrasound guided electrode insertion into the SPN with ultrasound localisation of the SPN to assist a more traditional iterative insertion process.

In addition to optimising our microneurography technique, we also tested the feasibility of an alternative amplifier/data acquisition system. Classically, microneurographic recordings have been made with 'home made' amplifiers and analogue to digital converters. Alternatively, commercial acquisition systems are available e.g. NeuroAmp EX from ADI instruments. The first option requires considerable technical expertise and support. The second option, as noted previously (Glover et al. , 2017), has associated higher costs and experimental flexibility is potentially constrained by closed-source software; which is required for commercial viability. These issues are not unique to

microneurography and the neuroscience community has increasingly begun to adopt open-source hardware and software tools. One such project is Open Ephys, who have developed inexpensive hardware and freely available source code for electrophysiological data acquisition and analysis (webpage: http://www.open-ephys.org or wiki: https://open-ephys.atlassian.net/wiki/spaces/OEW/overview) (Siegle et al. , 2017). This hardware/software combination has been widely adopted for animal neurophysiology studies and recently protocols for its use for EEG recordings in humans have been published (Black et al. , 2017, Hermiz et al. , 2016). To our knowledge this system has not been used for human microneurography where it may offer advantages.

We demonstrate that ultrasound guidance, combined with an open source data acquisition system, for microneurography facilitates identification and recording of nerves to increase data yield. This has the potential to broaden the utility of autonomic and sensory microneurography by enabling targeting of deeper nerves or smaller peripheral nerves as required by the scientific hypothesis under test or by the clinical presentation of a patient.

2. Methods

Experiments were conducted in accordance with The Code of Ethics of the World Medical Association (Declaration of Helsinki) for experiments involving humans. Ethical permissions were obtained from the Faculty of Biomedical Sciences Research Ethics Committee at the University of Bristol (ethics reference number: 51882). Written informed consent was obtained from all participants. Experiments were performed at the Clinical Research and Imaging Centre, University of Bristol, UK.

32 healthy volunteers (F:M 22:10, age range 19-34yrs) participated in these experiments. No subjects reported a history of neurological disease. Thermal thresholds for the lower leg (L5 dermatome), assessed with a contact thermode (Medoc TSA-II, Israel), were all in the normal range: cold detection 29.2±1.6˚C, warm detection 36.1±2.5˚C and heat pain 42.9±3.2˚C (mean ±SD from a baseline of 32˚C).

Participants were seated comfortably in a reclining bed. The right leg was supported with pillows and blankets such that it was kept relatively still and access to the recording site(s) were optimised. The skin over the recording site was cleaned with chlorhexidine, the electrodes were sterilised by prior autoclaving and a no touch technique was employed. A reference electrode (UNA35FRS, FHC, Maine, USA.) was inserted subcutaneously near the planned recording site.

In experiments targeting the common peroneal nerve (CPN), the nerve was identified by palpation proximal and lateral to the head of the fibula. The nerve was stimulated transcutaneously using a monopolar steel search cathode with an ECG electrode placed on the medial aspect of the knee as the anode. Pulsatile current stimulation (0.5ms duration, 0-10mA, and 0.5Hz) was applied to the skin overlaying the nerve until dorsiflexion of the ankle was evoked (using a DS7, Digitmer, Welwyn Garden City, UK and a PulsePal, open source stimulus generator, Sanworks, New York, USA). The current was reduced to identify the location where the least stimulus evoked a response; this point was then marked with a pen. The nerve was mapped in this

manner over two to three centimetres proximal to the fibular head. The recording electrode (200 µm diameter, 35mm length, tungsten, high impedance – 'No Zap'; UNA35FNS FHC, Maine, USA.) was then inserted into the nerve. Successful neural recording was detected by the characteristic insertion discharge associated with the ability to evoke 'mass activity' with gentle mechanical stimuli over the skin receptive field. The time from inserting the needle into the skin to successful neural recordings was measured (Skin to Nerve time). If mass activity indicating successful nerve recording was not found within 60 minutes of searching, the experiment was abandoned.

The superficial peroneal nerve (SPN) was located using a Toshiba Aplio 500 Ultra Sound scanner with a PLT-1204BT linear transducer (used at high frequency - 18MHz (Granata et al. , 2016)). We were guided by the sono-anatomy of the SPN as described previously (Canella et al. , 2009, Chin, 2013). Use of the ultrasound removed the need for electrical search stimulation. An insertion site in the distal half of the lateral lower limb was chosen: before the SPN pierces the crural fascia where the nerve was clearly visualised (but was not palpable); and free from blood vessels within the expected needle trajectory (Figure 1). The ultrasound probe was covered with a sterile transparent dressing and coated with sterile ultrasound gel. The recording electrode was inserted either with direct real-time ultrasound guidance (i.e. identifying the electrode subcutaneously and then advancing the tip intra-neurally under direct vision - Ultrasound (US) Guided) or after visualisation of the nerve and marking of the skin and without further use of ultrasound (Ultrasound (US) Located).

The recording and stimulating arrangement is shown in Figure 1A. Signals from the micro-electrodes were amplified with an Intan RHD2216 chip (Intan Technologies, Los Angeles, USA.) placed close to the recording site and grounded via an earth plate positioned on the calf distal to the recording site. The signal was digitised on the INTAN chip at 30kHz and relayed to an Open Ephys (http://www.open-ephys.org) acquisition board. The data was displayed via the Open Ephys GUI (http://www.open-ephys.org/gui/) on a laptop computer. The digital bandpass filter was set at 300-4000Hz . The neurogram was also output as an audio signal via the laptop speakers. During data acquisition, the laptop was powered from its internal battery and the acquisition board was powered via a USB Power bank battery (rating of 20,000 mA hrs, Aukey, https://www.aukey.com).

When successful neural recordings were obtained, the cutaneous innervation territory was searched for slowly conducting afferents using transcutaneous stimulation with a steel electrode of either 1mm or 5mm diameter tip. This search often started in a region identified by the subject as being the site of origin of the transient paraesthesia elicited by the electrode advancement. The latency to spike discharge following electrical stimulation of the receptive field was noted and this latency was divided by the distance between stimulation and recording electrodes to generate conduction velocities. When slowly conducting afferents had been identified (conduction velocities < 1.5m/s), sterile electro-acupuncture needles (Harmony Medical Classic Original Acupuncture Needles 13mm Length - 0.22mm Diameter) were inserted intradermally, immediately distal and advanced to within 5mm of the electrical receptive field. C fibres were stimulated (0.125-2Hz, 0.5ms duration, 0-20mA (Digitimer DS7 driven by PulsePal)) at increasing frequency to determine the extent of their activity dependent slowing (ADS). The

protocol to elicit ADS was as per Obreja et al., 2010 (Obreja et al. , 2010). The PulsePal was controlled via Matlab (2016a, Mathworks); stimulation current output was recorded by Open Ephys in parallel with neural recordings. The stimulation protocol consisted of a 2 minute pause in stimulation followed by 20 consecutive stimulations each at 0.125 Hz, 0.25 Hz, and 0.5Hz. This was then followed by a further 2 minute pause and then either 2 or 3 minutes of stimulation at 2 Hz with 60 stimulations at 0.25 Hz.

Sensory afferent data were analysed in Matlab. Spike thresholds were determined manually to exclude noise and were approximately +/- 10 μV. All threshold crossings following stimulation were then plotted as their latency after the stimulus against the time of the stimulus. Characteristic constant latency threshold crossings, which slowed with increasing stimulus frequency, could then be recognised as likely C nociceptor action potentials (Gee et al. , 1996, Serra et al. , 1999) These were then isolated from the noise using the Matlab function Selectdata. Isolation of these characteristic latency responses then allowed for isolation of the individual action potential profiles. These were overlaid and average waveforms generated. Constant latency responses were also visualised via "waterfall plots" (Torebjork and Hallin, 1974) where sequential raw data traces following cutaneous stimulation are plotted. Example Matlab scripts are available from the corresponding author on request.

To test whether ultrasound guidance could confer an advantage when attempting to access a challenging site for microneurography, we made recordings from the right phrenic nerve in the neck (AEP – last author (age 53yrs, male)). The phrenic can be visualised deep to the sternocleidomastoid and superficial to the anterior scalene muscle. It runs lateral to medial as the probe is moved caudally. It is often visualised during interscalene brachial plexus blocks for regional anaesthesia of the upper limb. Indeed, it is often inadvertently blocked by this technique (https://www.nysora.com/ultrasound-guided-interscalene-brachial-plexus-block-2017).

The participant lay supine with their head turned to the left. The Aplio ultrasound scanner was used to visualise the nerve at a site 2 cm rostral to the clavicle. At this point: the probe could be held comfortably with good quality images; there was large separation between the phrenic nerve and the brachial plexus and there were no overlying blood vessels. The insertion site was cleaned with 2% chlorhexidine. The reference electrode (UNA35FRS – as for the lower limb nerves) was inserted over the mastoid process to minimise EMG interference. The recording electrode (UNA35FNS) was inserted lateral to medial and in-plane. The insertion of the electrode to the nerve was uneventful and caused minimal discomfort. With the recording electrode stably placed within the nerve, the subject performed a number of respiratory manoeuvres including increasingly large inspiratory efforts, Valsalva and held inspiration. ECG was simultaneously recorded (lead II) via self-adhesive ECG electrodes fixed to each shoulder and the signal was passed to the Intan Chip.

These data were converted into a binary file within Matlab (script available on request) and then imported into Spike2v7 (Cambridge Electronic Design). The raw nerve signal was digitally bandpass filtered (300Hz to 4kHz) and the ECG at (0.1 – 25Hz). Spike was

then used to display the data and to extract instantaneous phrenic firing rates (0.2second rolling average) and instantaneous heart rate.

All data were expressed as mean ± SEM unless otherwise stated. Times to successful nerve recordings were displayed as Kaplan Meier plots and analysed using the Mantel-Cox test to account for censored cases (where no recording was obtained within the pre-defined cut off period (Choi and Lam, 2017)). These analyses and comparisons of pain ratings were performed in Prism 5 (GraphPad, San Diego, USA).

3. Results and Discussion

The experimental interventions required to make the microneurographic recordings were generally well tolerated by the study participants and were completed in 88% of subjects (28/32). Four recordings were terminated early: one volunteer felt light headed following needle insertion into the nerve, one complained of pain on needle insertion and two were unable to stay sufficiently still to complete the experimental protocol. At follow up, one week after recordings, none of the subjects reported any persisting pain, discomfort, numbness or paraesthesia.

During our initial efforts to make cutaneous C nociceptor recordings, we found that recordings from the common peroneal nerve often yielded non-cutaneous afferents, i.e. from fibres belonging to the deep peroneal nerve (DPN). In total 63% (10/16) of recordings from the CPN yielded DPN afferents. We were therefore in a situation where we were finding nerve recordings time consuming to make and, when we could make recordings, the identified unit was not of the cutaneous subtype that we were seeking.

To improve our data yields we wished to target the SPN directly, however, its small size makes it challenging to record using conventional palpation and electrical stimulation methods (it has no muscle fascicles so no twitch is evoked although evoked paraesthesia could be used to identify electrode proximity). The sono-anatomy of the SPN is well characterised (Canella et al. , 2009, Chin, 2013) and it is commonly targeted during regional anaesthesia as part of an ankle block so we switched to attempting to use ultrasound to locate the nerve. The SPN was straightforward to locate on ultrasound scan (Figure 1, B and C). The time to identify the nerve with ultrasound was not specifically recorded, but we found this took only a couple of minutes maximum. Holding the SPN in the short axis view allowed the recording electrode to be advanced 'in plane' from the anterior aspect of the lower leg aiming posteriorly towards the nerve. This approach enabled visualisation of the recording electrode along an approach track of up to 1 cm of tissue to stabilise the electrode after insertion into the nerve (Figure 1). It is worth noting that the use of ultrasound removed the need to electrically stimulate the nerve whilst trying to locate its position. This both shortens the experiment duration and reduces the unpleasantness and stress for the participant.

Ultrasound guidance significantly increased the number of experiments resulting in successful nerve recordings. Furthermore it significantly reduced the time taken to achieve successful recordings. Success rates and median skin to nerve times improved from 80% and 28.5 minutes at the CPN (18 participants) to 100% and 4.5 minutes at the SPN(6 participants) ($P<0.0001$, Mantel-Cox log rank test, Figure 2A). Additionally, in comparison to using the ultrasound to only locate (Ultrasound (US) located) the SPN, full real-time ultrasound guidance (Ultrasound (US) guided) improved success rates from 20% (1 out of 5, with the time taken in that one success of 9 mins) to 100% with a median skin to nerve time of 7 (range 2-9) minutes ($P=0.005$, Mantel-Cox log rank test, Figure 2B). Therefore the use of ultrasound guidance was beneficial both in terms of time and yield of recordings from the peroneal nerve irrespective of the chosen comparator site.

No differences were found in the pain scores from the volunteers who participated in the experiments to compare ultrasound guidance to ultrasound location of the SPN:

Worst pain (0-10) ultrasound guided vs ultrasound located 3.4±1.2 vs 3.4±1.2 and average pain (0-10) 1.5±0.5 vs 1.4±0.2 respectively (n=5).

One concern that has been expressed about the use of ultrasound in microneurography was that it could not guarantee improved data yields, only increase the efficiency of placing the recording electrode into the nerve. It could also theoretically reduce the stability of the recordings if the recording electrode trajectory was altered to make insertion amenable to ultrasound guidance (McNulty and Hodson-Tole, 2016). Cutaneous C fibre nociceptors were identified in 9/13 experiments with ultrasound guidance within the SPN and 2/18 with the classic approach at the CPN. Often there were multiple constant C-fibre latencies within these recordings; presumably the electrode tip was in the vicinity of a Remak bundle. Though most often only one unit was identified with the transcutaneous stimulation and it was this unit that was the subject of further characterisation. The chosen unit was selected based on an amplitude that was sufficiently large to be identifiable by eye during stimulation, i.e. a signal:noise ratio of greater than ~1.5. We did not note any problems with stability. We held these units for 65 (50 – 85) minutes (mean (range)) both at the CPN and the SPN until the end of our study protocol. Only in one of these recordings was the unit lost prior to completion of the protocol. As the experiments were terminated at the end of the protocol, the upper range of our recording times does not represent maximal possible recording times. Importantly, we did not lose any recordings when removing the ultrasound probe from contact with the leg which might be expected to be the critical point.

An example of a C fibre nociceptor recording from the SPN using the Open Ephys acquisition system is shown in Figure 3. The shortest possible conduction distance was 0.18m giving an estimated initial conduction velocity of 0.9m/s. The degree of slowing from baseline in the C fibre during both low frequency (0.6% at 0.125Hz, 1.2% at 0.25Hz and 2.4% at 0.5Hz) and high frequency (~23% at 2Hz) stimulation suggests that this unit was nociceptive (Obreja et al. , 2010). The signal to noise ratio was sufficiently good to isolate the spike waveform from noise with a simple threshold crossing criterion to build the activity-dependent slowing (ADS) profile (figure 3A). Individual C fibre ADS profiles could then be selected from the raster plot and isolated for further analysis (Figure 3B); for example, average waveforms from the ADS period could be generated (Figure 3D). A 'waterfall' plot of raw data traces from sequential stimulations during 2Hz stimulation is also shown (Figure 3C). Figures 3C and 3D demonstrate the signal to noise ratios using the Open Ephys / Intan acquisition package. The baseline noise in this trace, of less than ± 10μV, is characteristic of the Open Ephys acquisition in our hands. It is of note that these experiments were not performed in an electrically shielded lab.

The complete Open Ephys acquisition system with Intan amplifier chip and the PulsePal stimulus generator, cost approximately £4000. This compares well with equivalently specified commercially available systems. It offers potential performance advantages because of the on chip amplification and digitisation near the recording site which reduces noise/hum. In addition, the open source structure of the software provides an opportunity for customisation of algorithms for acquisition and analysis.

The utility of ultrasound guided microneurography in accessing difficult to reach nerves is demonstrated by the recordings made from the phrenic nerve. To the best of our knowledge this is the first report of such a recording. The gross and ultrasound anatomy of the approach is shown in Figure 4 A and B. The multi-unit phrenic nerve activity (Figure 4C) shows a ramping pattern with amplitude graded according to increasing respiratory effort which is maximal during a modified Valsalva manoeuvre (with accompanying heart rate changes). The recording was stably and comfortably held during these manoeuvres for a period of almost an hour.

Prior to undertaking our recordings from the phrenic nerve we performed a risk assessment. Microneurography has an excellent safety record with no long term motor or sensory abnormalities reported when conducted by trained specialists with appropriate care and consideration. We do know that microneurography carries < 10% risk of paraesthesia lasting 2-10 days (Eckberg et al. , 1989, Gandevia and Hales, 1997, Vallbo, 2018). When applied to the phrenic nerve, we assessed that the worst possible outcome of microneuorography could be a hemi-diaphragm palsy such as those reported (relatively commonly) with brachial plexus regional anaesthesia (El-Boghdadly et al. , 2017). Other anticipated adverse outcomes included hiccoughs and pain. A resolving hemi-diaphragm palsy is only of clinical relevance in patients with underlying respiratory disease as, “In healthy individuals, ….. tidal volumes remain unchanged due to a greater contribution from the rib cage” (El-Boghdadly et al. , 2017). Therefore, although phrenic palsy was our worst case scenario, we anticipated that it was very unlikely (given the low incidence of such palsies with microneurography at other sites) and that even should it occur then it would be unlikely to cause respiratory compromise in an otherwise healthy volunteer subject. To further mitigate risk, our experiments were performed in a clinical research institute that has full resuscitation facilities. In this case the recording proceeded uneventfully, was easily tolerated and produced no short or long term sequalae. Nonetheless we recommend that any efforts to repeat such phrenic recordings proceed only in the context of appropriate risk assessment and mitigation.

As demonstrated here, ultrasound guidance, combined with open source data acquisition systems has the potential to simplify the adoption and broaden the scope of autonomic and sensory microneurography; enabling targeting of deeper nerves or smaller peripheral nerves as required by the scientific hypothesis under test or by the clinical presentation of a patient.

4. Conclusions and Significance

We have demonstrated quantitatively that ultrasound guided electrode insertion in sensory microneurography improves both data yields and productive experimental time. It should be noted that we have examined the benefits of ultrasound in the hands of a relatively inexperienced microneurographer (JPD, 5 months previous training in an established microneurography lab) and in the context of establishing the technique of sensory microneurography from scratch in our laboratory. Based on our experience we anticipate that novice microneurographers may find benefit in using ultrasound to locate their target nerves in that it may shorten their learning curve and give them more real time feedback information on which to develop their practice.

We have also provided evidence that the Open Ephys electrophysiological data acquisition system is suitable for microneurography and enables low noise, stable recordings. The recording system is cost effective compared to commercially available microneurography systems, is relatively portable and, as the software is open source it can be modified to meet the needs of the research community.

In a single individual, we have performed a proof of principle study which demonstrates the utility of ultrasound guidance in targeting the phrenic nerve, which has previously been considered inaccessible to microneurography. This approach was well tolerated and demonstrated the classical physiology as expected from prior animal work.

In future studies we hope that ultrasound guidance will not only improve experiment efficiency, but will also facilitate targeting of previously 'challenging' nerves as dictated by the specific research question or by clinical presentation: for example small cutaneous nerves with distal neuromas or deep muscle innervation. As such even experienced microneurographers may find it of use to access new target nerves and facilitate patient studies.

5. Acknowledgements

Dr. Kenneth K. F. Ho: ONLINE MRI & CT SECTIONAL ANATOMY, http://omcsa.org. For the MRI images included in figure 1.

None of the authors have potential conflicts of interest to be disclosed.

Figure 1 - Ultrasound guided placement of the microneurography recording electrode in the superficial peroneal nerve.

A. Diagrammatic representation of the experiment. The high frequency linear ultrasound probe is placed lateral to the shin over the superficial peroneal nerve (SPN) with its long axis oriented anterior-posterior allowing visualisation of the recording electrode in plane (see panel B). The signal from the active and reference electrodes are amplified and digitised by the Intan RHD2216 chip, positioned close to the recording site. The digitised signal is relayed via the Open Ephys acquisition box before being displayed and stored on a battery powered laptop. The laptop computer also runs Matlab 2016b which drives the PulsePal stimulus generator triggering the DS7 constant current stimulator. This stimulation is delivered to the cutaneous receptive field of the C fibre on the dorsum of the foot via fine intradermal needles.

B. Images obtained during ultrasound guided needle insertion (structures annotated below). The electrode can be seen in the long axis entering superficially and anteriorly in the top left of the panel towards the hyper-echoic SPN (~5mm diameter with visible nerve fascicles). The SPN is flanked anteriorly by extensor digitorum longus (EDL) and posteriorly by the peroneus muscles (PM). The fibula can be seen deep to PM in the bottom right of the panel.

C. Cross sectional MR image of the lower leg for reference showing the relative positions of the lateral structures visualised with the ultrasound. Note the superficial location of the SPN.

Figure 2 – Ultrasound guidance in microneurography improves data yields and reduces time to successful recordings.

A. Kaplan Meier plot comparing time to successful recordings with a classic approach to the Common Peroneal Nerve (using surface landmarks, palpation and electrical stimulation to localise) to an ultrasound-guided approach to the Superficial Peroneal Nerve. The classic approach was used in 18 volunteers and the ultrasound-guided in 6. Median times to successful recordings were 4.5mins for ultrasound guided vs 28.5 minutes for the classic approach ($P<0.0001$ Mantel-Cox, Log-rank Test). Ultrasound guidance led to a 100% success rate vs 80% with the classic approach (within a 1 hour permissible search window).

B. Insertion of the recording electrode with real-time ultrasound guidance improves yield. In 5 volunteers, the time to successful nerve recordings were compared when using direct vision to guide placement of the recording electrode (ultrasound (US) Guided) vs using ultrasound to simply locate the nerve, marking the skin and then placing the electrode iteratively (ultrasound (US) Located). Ultrasound guidance led to a 100% success rate vs 20% with the iterative approach. These survival curves are significantly different ($P<0.005$ Mantel-Cox, Log-rank Test). The median time to successful recording was 7 mins for ultrasound guided.

Figure 3 – Example neuronal recordings.

A. Example of activity dependent slowing (ADS) in a C fibre afferent. The conduction distance was at least 0.18m (conduction velocity of ~0.92m/s). The left Y axis shows latency to threshold crossings following cutaneous electrical stimulation (black dots). The right Y axis shows the frequency of stimulation (red dots). ADS is evoked in the C fibre with an initial latency of ~0.19s with low frequency (0.125, 0.25 and 0.5Hz) and then to a greater extent with 2Hz stimulation Recovery from ADS is demonstrated during subsequent 0.25Hz stimulation. Note that a second more slowly conducting afferent is also seen to be slowing during 2Hz stimulation at a latency of 0.26 to 0.28s.

B. Following extraction using Matlab, the ADS in the now isolated C fibre is more clearly shown. The unit slows 0.6% at 0.125Hz, 1.2% at 0.25Hz, 2.4% at 0.5Hz and 23% at 2Hz. The vertical grey rectangle shows those sweeps displayed in panel C

C. Sequential raw data sweeps from 0.18s after the stimulation to 0.3s after the stimulation (x axis) are shown. The earliest sweep is uppermost – labelled 1. The Y axis is voltage with a minima maxima of each sweep of -5 μV to +20 μV. Slowing of the C fibre action potential with 2 Hz stimulation is easily recognised (solid box). Furthermore, 2 additional likely C fibre action potentials are also seen (dotted boxes).

D. All of the action potentials identified from the single C fibre nociceptor are overlaid. The action potentials are centred upon their maximal deflection which is shown at 1ms. The mean voltage is shown as a solid black line bounded by the standard deviation shown as the paired black dashed line.

Note that the C fibres that we have identified have their major deflection in the negative direction as is expected from microneurographical recordings – the scale in figures 3C and 3D is inverted to show the more standard upward deflection.

Figure 4 - Ultrasound guided phrenic nerve recordings.

A. Schematic of a dissection of the right side of the neck showing the relations of the major blood vessels (internal jugular vein – I.J.V. and common carotid artery), the anterior scalene muscle (A.S.) and the phrenic nerve passing from rostral and lateral to caudal and medial over the A.S. The black rectangle represents the approximate position of the ultrasound probe.

B. Ultrasound image during electrode placement into the phrenic nerve. The orientation of the image is as shown in A. The phrenic nerve can be seen in transverse section in the centre of the image, highlighted with a yellow circle. The diameter is of the order of 1 mm. It lies superior and medial to the AS and inferior to the sternocleidomastoid muscle (SCM). The electrode can be seen just entering the nerve – highlighted in the dashed red rectangle.

C. Phrenic nerve recording.
Multi-unit phrenic nerve activity (with average spike rate) and ECG with heart rate during periods of tidal ventilation (TV), an inspiratory hold (TV hold), maximal inspiration (Max I) and a Valsalva with forced expiration against a closed glottis. Each inspiratory period is marked with a vertical bar. Note the augmenting pattern of phrenic discharge in inspiration and the maintained activity during an inspiratory hold and during the Valsalva manoeuvre early phase.

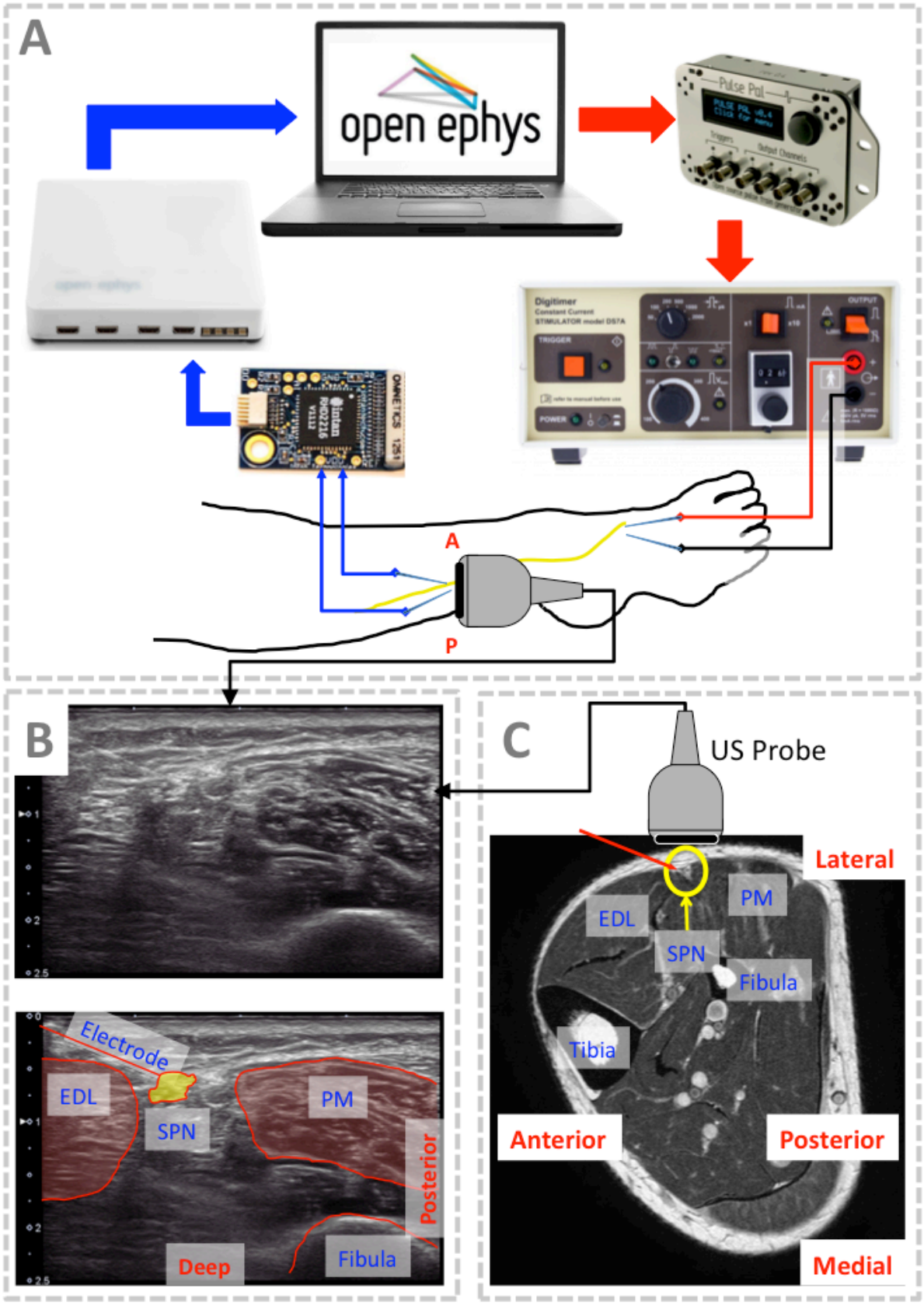
A
open ephys
Pulse Pal
Digitimer
Constant Current
STIMULATOR model DS7A
TRIGGER
OUTPUT
POWER
A
P
B
Electrode
EDL
SPN
PM
Posterior
Deep
Fibula
C
US Probe
Lateral
PM
EDL
SPN
Fibula
Tibia
Anterior
Posterior
Medial

A Plot of time to obtain nerve recordings.

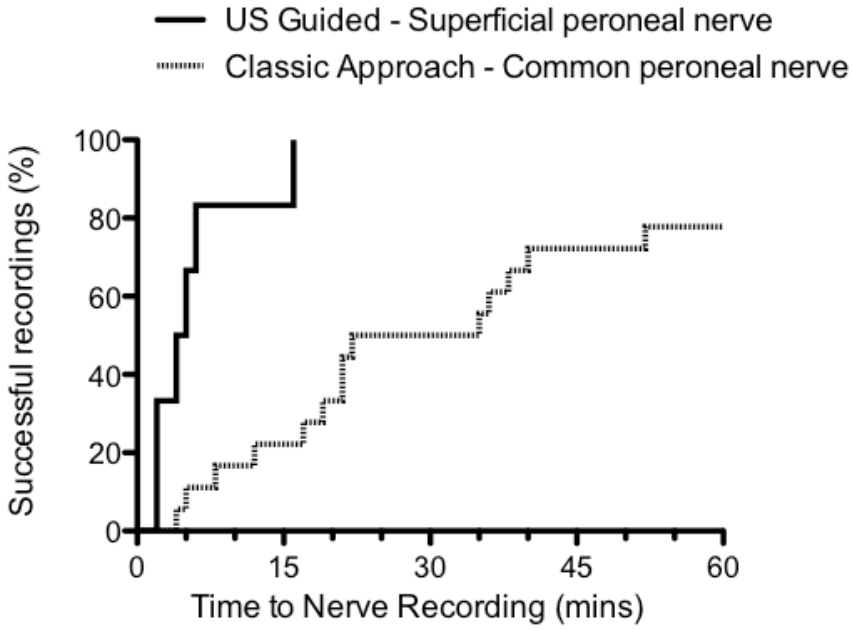

B Plot of time to obtain nerve recording:
US guidance vs US localisation.

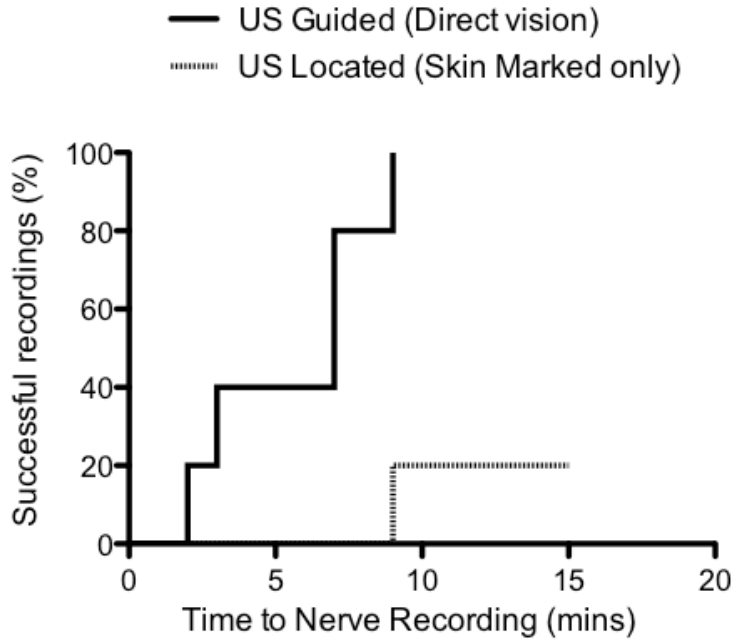

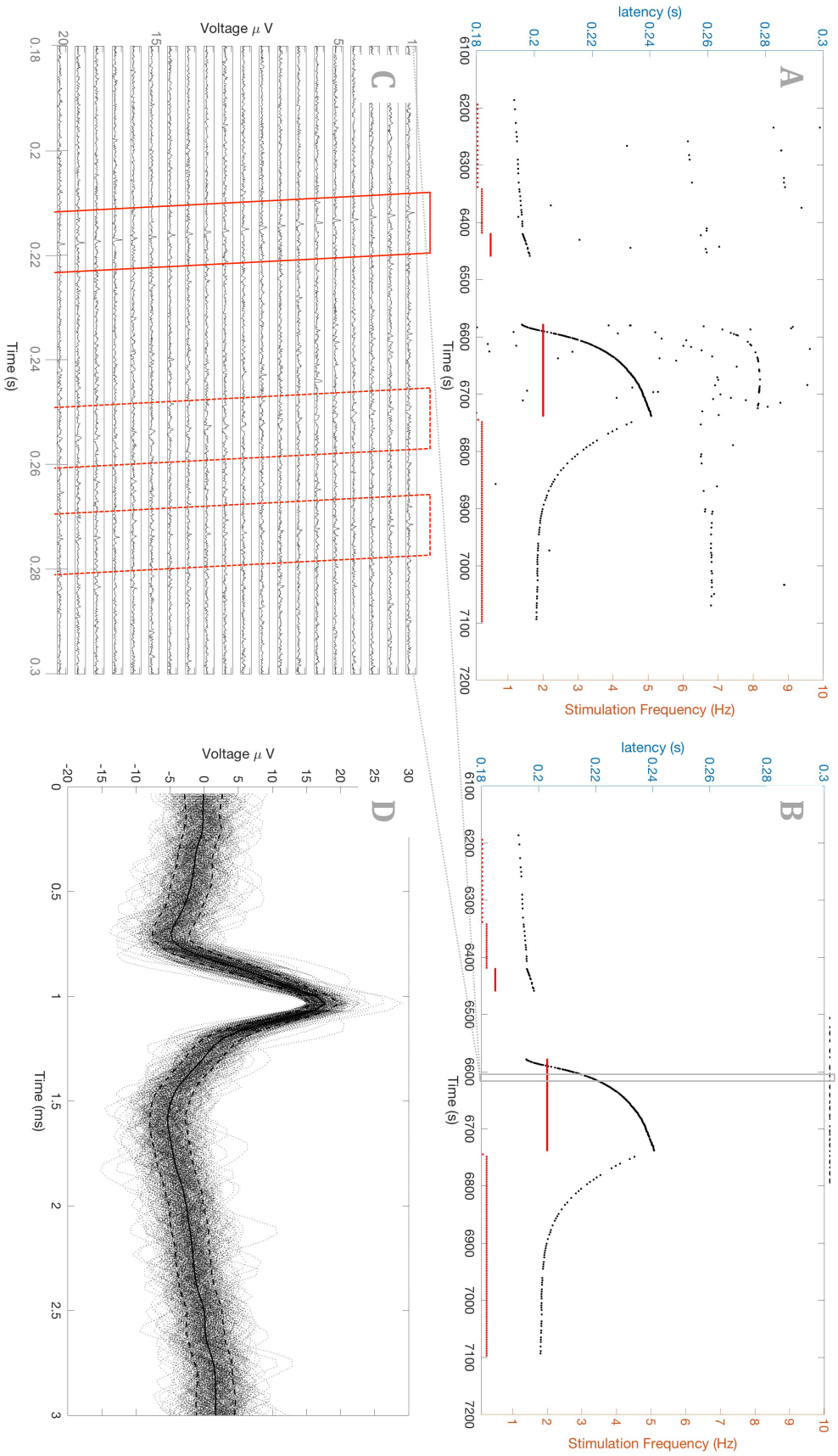
A
latency (s)
Time (s)
Stimulation Frequency (Hz)
B
latency (s)
Time (s)
Stimulation Frequency (Hz)
C
Voltage μ V
Time (s)
D
Voltage μ V
Time (ms)

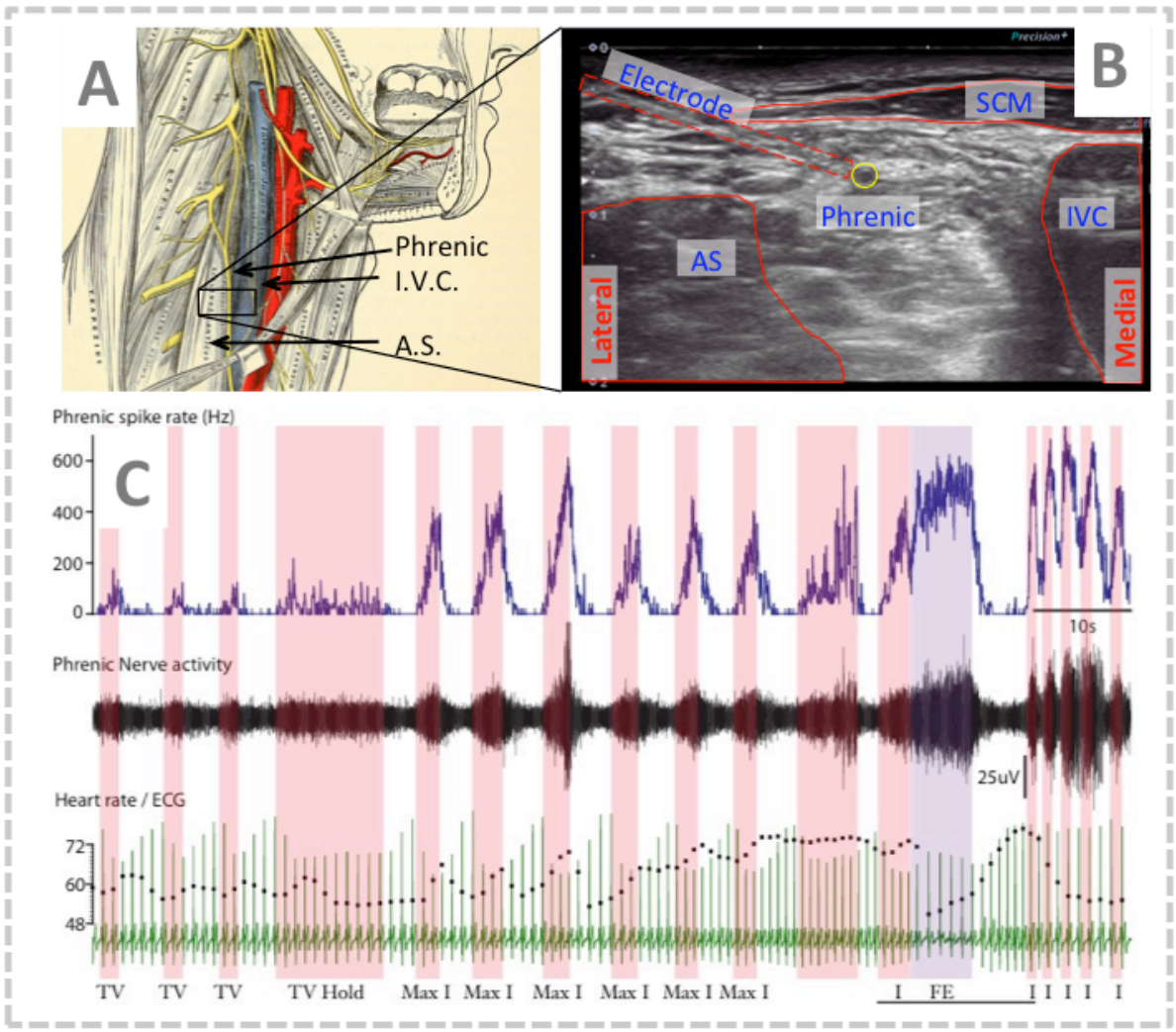
A
Phrenic
I.V.C.
A.S.
B
Electrode
SCM
Phrenic
IVC
AS
Lateral
Medial
Phrenic spike rate (Hz)
C
600
400
200
0
10s
Phrenic Nerve activity
25uV
Heart rate / ECG
72
60
48
TV TV TV TV Hold Max I Max I Max I Max I Max I Max I I FE I I I I I

6. Bibliography

Black C, Voigts J, Agrawal U, Ladow M, Santoyo J, Moore C, et al. Open Ephys electroencephalography (Open Ephys + EEG): a modular, low-cost, open-source solution to human neural recording. Journal of neural engineering. 2017;14:035002.
Canella C, Demondion X, Guillin R, Boutry N, Peltier J, Cotten A. Anatomic study of the superficial peroneal nerve using sonography. American journal of roentgenology. 2009;193:174-9.
Chin KJ. Ultrasound visualization of the superficial peroneal nerve in the mid-calf. Anesthesiology. 2013;118:956-65.
Choi SW, Lam DMH. Comparing times in clinical studies with a finite ending. Anaesthesia. 2017;72:1554-6.
Curry TB, Charkoudian N. The use of real-time ultrasound in microneurography. Autonomic neuroscience : basic & clinical. 2011;162:89-93.
Donadio V, Liguori R. Microneurographic recording from unmyelinated nerve fibers in neurological disorders: an update. Clinical neurophysiology : official journal of the International Federation of Clinical Neurophysiology. 2015;126:437-45.
Eckberg DL, Wallin BG, Fagius J, Lundberg L, Torebjork HE. Prospective study of symptoms after human microneurography. Acta Physiol Scand. 1989;137:567-9.
El-Boghdadly K, Chin KJ, Chan VWS. Phrenic Nerve Palsy and Regional Anesthesia for Shoulder Surgery: Anatomical, Physiologic, and Clinical Considerations. Anesthesiology. 2017;127:173-91.
Gandevia SC, Hales JP. The methodology and scope of human microneurography. J Neurosci Methods. 1997;74:123-36.
Gee MD, Lynn B, Cotsell B. Activity-dependent slowing of conduction velocity provides a method for identifying different functional classes of c-fibre in the rat saphenous nerve. Neuroscience. 1996;73:667-75.
Glover PM, Watkins RH, O'Neill GC, Ackerley R, Sanchez-Panchuelo R, McGlone F, et al. An intra-neural microstimulation system for ultra-high field magnetic resonance imaging and magnetoencephalography. J Neurosci Methods. 2017;290:69-78.
Granata G, Giambattistelli F, Padua L, Coraci D, Petrini FM. High-frequency ultrasound in guiding needle insertion for microneurography. Clinical neurophysiology : official journal of the International Federation of Clinical Neurophysiology. 2016;127:970-1.
Hermiz J, Rogers N, Kaestner E, Ganji M, Cleary D, Snider J, et al. A clinic compatible, open source electrophysiology system. Conference proceedings : Annual International Conference of the IEEE Engineering in Medicine and Biology Society IEEE Engineering in Medicine and Biology Society Annual Conference. 2016;2016:4511-4.
McNulty PA, Hodson-Tole EF. Letter in response to "High-frequency ultrasound in guiding needle insertion for microneurography" by Granata and colleagues. Clinical neurophysiology : official journal of the International Federation of Clinical Neurophysiology. 2016;127:1737-8.
Obreja O, Ringkamp M, Namer B, Forsch E, Klusch A, Rukwied R, et al. Patterns of activity-dependent conduction velocity changes differentiate classes of unmyelinated mechano-insensitive afferents including cold nociceptors, in pig and in human. Pain. 2010;148:59-69.
Serra J, Campero M, Bostock H, Ochoa J. Two Types of C Nociceptors in Human Skin and Their Behavior in Areas of Capsaicin-Induced Secondary Hyperalgesia. J Neurophysiol. 2004;91:2770-81.

Serra J, Campero M, Ochoa J, Bostock H. Activity-dependent slowing of conduction differentiates functional subtypes of C fibres innervating human skin. J Physiol. 1999;515 (Pt 3):799-811.
Siegle JH, Lopez AC, Patel YA, Abramov K, Ohayon S, Voigts J. Open Ephys: an open-source, plugin-based platform for multichannel electrophysiology. Journal of neural engineering. 2017;14:045003.
Torebjork HE, Hallin RG. Identification of afferent C units in intact human skin nerves. Brain research. 1974;67:387-403.
Vallbo AB. Microneurography - how it started and how it works. Journal of neurophysiology. 2018.
Vallbo AB, Hagbarth KE. Activity from skin mechanoreceptors recorded percutaneously in awake human subjects. Exp Neurol. 1968;21:270-89.
Vallbo AB, Hagbarth KE, Wallin BG. Microneurography: how the technique developed and its role in the investigation of the sympathetic nervous system. J Appl Physiol. 2004;96:1262-9.